

# Quantification of intergranular exchange coupling in CoPtCr-based perpendicular recording media via ferromagnetic resonance measurements

Daniel Richardson, Kumar Srinivasan, Sidney Katz, and Mingzhong Wu

Citation: [Appl. Phys. Lett.](#) **111**, 183506 (2017);

View online: <https://doi.org/10.1063/1.4990949>

View Table of Contents: <http://aip.scitation.org/toc/apl/111/18>

Published by the [American Institute of Physics](#)

---

---



## SciLight

Sharp, quick summaries **illuminating**  
the latest physics research

Sign up for **FREE!**



# Quantification of intergranular exchange coupling in CoPtCr-based perpendicular recording media via ferromagnetic resonance measurements

Daniel Richardson,<sup>1</sup> Kumar Srinivasan,<sup>2</sup> Sidney Katz,<sup>1</sup> and Mingzhong Wu<sup>1,a)</sup>

<sup>1</sup>Department of Physics, Colorado State University, Fort Collins, Colorado 80523, USA

<sup>2</sup>Western Digital, San Jose, California 95131, USA

(Received 19 June 2017; accepted 20 October 2017; published online 2 November 2017)

Intergranular exchange fields in CoPtCr granular media materials were quantified through ferromagnetic resonance measurements in various magnetic states. The data indicate that the exchange field in CoPtCr granular films with no oxide segregant is comparable to the saturation magnetization of the films. With an introduction of a SiO<sub>2</sub> segregant, however, the exchange field decreases. A 30% volume fraction of the segregant reduces the strength of the intergranular exchange coupling to zero. *Published by AIP Publishing.* <https://doi.org/10.1063/1.4990949>

Perpendicular magnetic recording (PMR) using CoCrPt-oxide granular media has recently achieved areal storage densities close to 1 Tb/in.<sup>2</sup>.<sup>1,2</sup> While PMR media technology has matured, there is still a great need to better understand the physics behind the granular media, which is very important not only for the current PMR technology to realize densities beyond 1 Tb/in.<sup>2</sup> but also for the next-generation heat assisted magnetic recording (HAMR) in which granular media are heated to elevated temperatures during the writing process. Physics questions of great significance, for example, are how the oxide segregant in the media affects the grain size and the grain properties and thereby the thermal stability<sup>3–5</sup> and how it affects the strength of the effective field experienced by individual grains and thereby influences the signal-to-noise ratio during reading.<sup>6–8</sup>

In addition to the external writing field, an individual grain in the PMR media experiences a uniaxial magnetocrystalline anisotropy field, a self-demagnetization field, an effective dipolar interaction field due to other grains, and an intergranular exchange field. The anisotropy and demagnetization fields can be determined relatively easily through conventional measurement techniques such as vibrating sample magnetometer (VSM) and ferromagnetic resonance (FMR) techniques, but the accurate determination of the effective dipolar and exchange interaction fields is rather challenging. Some indirect methods, such as the so-called  $\Delta H_c$  method (difference in the coercivities of full hysteresis loops and minor recoil loops),<sup>9–11</sup> the first-order reversal curve (FORC) approach,<sup>12</sup> the differential remnant curve approach,<sup>13–16</sup> and the demagnetizing factor compensation method,<sup>17–19</sup> have been used to examine the dipolar and exchange interactions in PMR media, mostly through switching field distribution measurements. However, those methods are limited because they either rely on a certain set of assumptions or do not incorporate all the material details, and each method alone does not yield accurate results.<sup>20</sup>

This letter reports on the study of intergranular exchange coupling in PMR media through the determination of effective exchange fields for different remnant magnetic states via FMR measurements. The effective exchange field  $H_{ex}$

increases linearly with a decrease in the remnant magnetization  $M_r$ . The extrapolation of the  $H_{ex}$  vs.  $M_r$  plot to the  $H_{ex}$  axis yields the intrinsic intergranular exchange field. This FMR approach was first used by Hinata *et al.* to compare the exchange fields in two media samples prepared using different argon pressures.<sup>21</sup> In this work, it is used to investigate systematically the effects of the oxide segregant on the intergranular exchange interactions in PMR media. The data show that the intrinsic exchange field in CoPtCr granular films is about the same as the saturation induction and about half of the perpendicular anisotropy field. With the introduction of the SiO<sub>2</sub> segregant to the films, the exchange field decreases. It decreases to zero when the volume fraction of the SiO<sub>2</sub> segregant is increased to 30%. These results, together with others presented shortly, contribute to the understanding of intergranular exchange coupling in PMR media.

The study made use of four CoPtCr-based granular film samples with different amounts of SiO<sub>2</sub> segregant. The samples are 4-mm-diameter circular elements cut from 2-in.-diameter media disks that were grown by magnetron sputtering. The static magnetic properties of the samples were determined through VSM, magneto-optical Kerr effect (MOKE), and standard FMR measurements and are presented in Fig. 1.

Figures 1(a) and 1(b) show the effective saturation induction  $4\pi M_s$  and the effective perpendicular anisotropy field  $H_k$ , respectively, as a function of the volume fraction  $x$  of the SiO<sub>2</sub> segregant. One can see from the data that the introduction of 10% SiO<sub>2</sub> into the CoPtCr film leads to a slight increase in  $4\pi M_s$  and a notable increase in  $H_k$ . This results mainly from the improvement of the composition gradient from the grain centers to the grain boundaries in the PMR media.<sup>22</sup> In more details, the introduction of the oxide segregant into the grain boundaries leads to the migration of the non-magnetic elements (Pt and Cr) from the grain cores to the grain boundaries, resulting in a higher magnetization and stronger anisotropy in the grain cores. The increase in the core magnetization gives rise to a slight increase in the  $4\pi M_s$  value of the sample, even though the overall volume fraction of the magnetic phase is reduced. The enhancement in the core anisotropy is responsible for the increase in  $H_k$ . An increase in  $x$  from 10% to 20% gives rise to relatively

<sup>a)</sup> Author to whom correspondence should be addressed: [mwu@colostate.edu](mailto:mwu@colostate.edu)

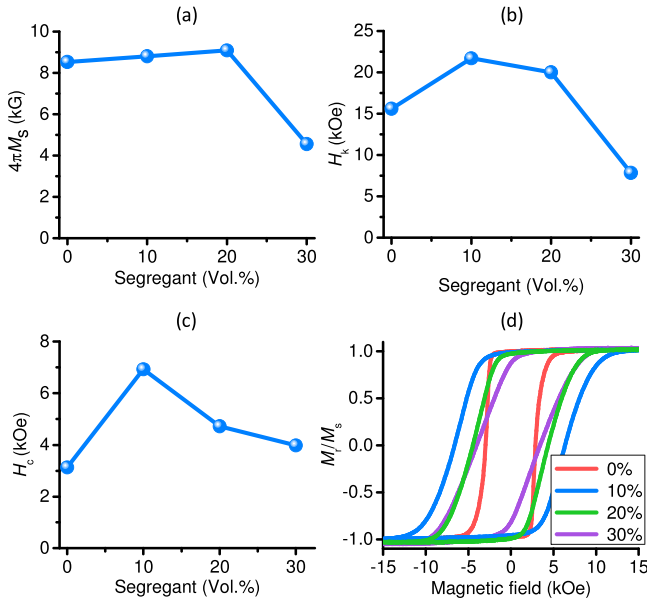


FIG. 1. Static magnetic properties of the samples. (a)–(c) The saturation induction  $4\pi M_s$ , effective perpendicular anisotropy field  $H_k$ , and coercivity  $H_c$  as a function of the volume fraction of the  $\text{SiO}_2$  segregant. (d) The magnetic hysteresis loops of the four samples, where the vertical axis shows the remnant magnetization  $M_r$  to saturation magnetization  $M_s$  ratio.

insignificant changes:  $4\pi M_s$  increases slightly while  $H_k$  decreases slightly. This indicates that the effects of adding 20%  $\text{SiO}_2$  are similar to those of adding 10%  $\text{SiO}_2$ . A further increase to 30%, however, results in rather significant drops in both  $4\pi M_s$  and  $H_k$ . There are two main reasons for this observation. First, a high- $x$  segregant gives rise to a reduction in the grain size, simply due to the segregant-produced constraint of space. Smaller grains are less thermally stable, resulting in a decrease in the  $4\pi M_s$  and  $H_k$  values of the sample. Second, the presence of a high- $x$   $\text{SiO}_2$  segregant also leads to the partial oxidation of the grains,<sup>22,23</sup> degrading their magnetic properties.

Two important points should be made about the above discussions. First, qualitatively it is well understood that the above-described change of the magnetic properties with an

increase in  $x$  should be accompanied by a drop in  $H_{\text{ex}}$ . However, quantitative studies about this have not been carried out yet. Such studies are presented below. Second, when the volume fraction of the oxide segregant is very large, the segregant enters deeply into the grain cores and thereby splits the grains into closely spaced, exchange-coupled, smaller sub-grains or even clusters.<sup>24</sup> This will result in a lower effective magnetization and a lower effective anisotropy field, just as in the above-discussed sample with  $x = 30\%$ , as well as enhanced exchange coupling. As presented shortly, the  $x = 30\%$  sample shows very weak exchange coupling, indicating no segregant-caused grain splitting in the sample.

Figure 1(c) presents the coercive field  $H_c$  as a function of  $x$ . The data show a trend which is similar to the change of  $H_k$  with  $x$  shown in Fig. 1(b). This similarity is expected because the magnetization switching in the PMR media largely depends on the strength of the perpendicular anisotropy. Figure 1(d) presents the full hysteresis loops of the four samples measured by the MOKE technique, from which the  $H_c$  data in Fig. 1(c) were determined. One can see that the sample with  $x = 0$  shows a nice square loop. The samples with  $x \neq 0$  show similar loops but with a squareness much lower than that of the  $x = 0$  sample.

The intergranular exchange field  $H_{\text{ex}}$  in the samples was measured using the experimental configuration sketched in Fig. 2(a) and the measurement steps illustrated in Fig. 2(b). The experimental setup consists mainly of a co-planar waveguide (CPW) device and a vector network analyzer (VNA), and the sample is placed on the CPW with the media side facing the CPW structure and the substrate side facing up. The measurements involve the following three major steps. First, the sample is magnetized to saturation in an out-of-plane configuration using a large positive magnetic field. The corresponding magnetization state in the hysteresis loop is indicated by point A in Fig. 2(b). Next, a moderate negative field is applied to switch some of the grains from the “up” state to the “down” state. This step brings the magnetization state in the loop from point A to point B. Last, a smaller negative field, which points downward as shown in Fig. 2(a),

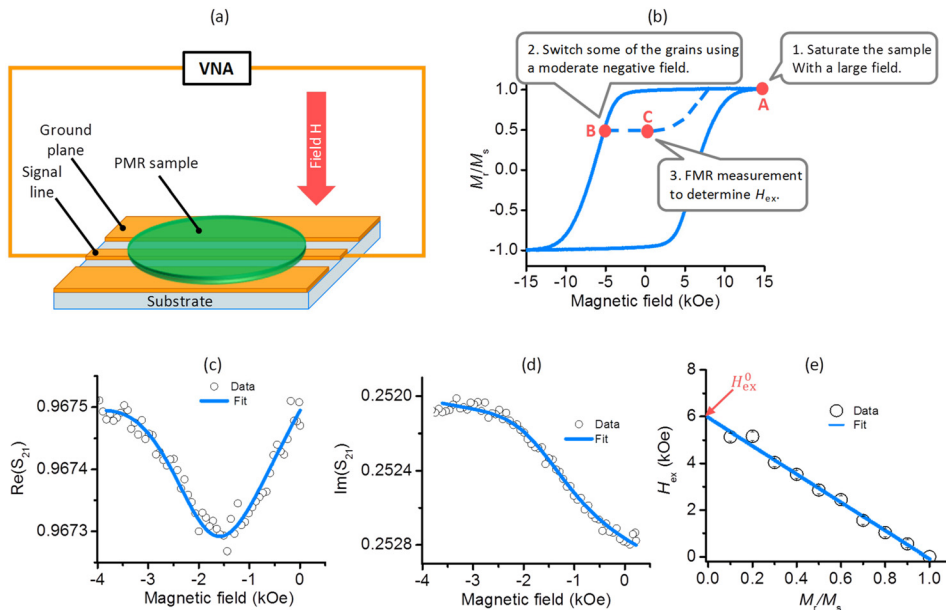


FIG. 2. Exchange field measurement approach. (a) Experimental configuration. (b) Major experimental steps. (c) and (d) The real and imaginary parts of the  $S_{21}$  parameter of the CPW/sample structure. The open circles show the data, while the blue curves show the numerical fits. (e) Effective exchange field  $H_{\text{ex}}$  as a function of  $M_r/M_s$ . The open circles present the data, while the line is a linear fit. The fitting yields the intrinsic exchange field  $H_{\text{ex}}^0$ , as indicated. All the data were obtained with the 10%-segregant sample.

is applied to change the magnetization state from point B to point C, and the FMR measurement is then performed by sweeping the external field about this field and measuring the complex transmission parameter  $S_{21}$  of the CPW/sample structure with the VNA. During the FMR measurements, both the microwave frequency and power are kept constant.

By selecting the appropriate microwave frequency ( $f$ ), one can realize FMR for un-switched “up” grains, not switched “down” grains, in the media sample. For the FMR in those “up” grains, one can write the Kittel equation as

$$f = |\gamma|(H_{\text{FMR}} + H_{\text{eff}}), \quad (1)$$

where  $|\gamma|$  is the absolute gyromagnetic ratio,  $H_{\text{FMR}}$  is the external static magnetic field at which the resonance occurs, and  $H_{\text{eff}}$  is the effective internal field on the “up” grains and can be written as<sup>21</sup>

$$H_{\text{eff}} = H_k - N_g 4\pi M_s - (N_0 M_r - N_g 4\pi M_s) - H_{\text{ex}}, \quad (2)$$

where  $N_g$  is the demagnetization factor of an individual grain,  $N_0$  is the global demagnetization factor of the film sample, and  $M_r$  is the remnant magnetization. Note that for the data presented below, most of the FMR measurements were performed in a field region indicated by point C in Fig. 2(b) and  $H_{\text{FMR}}$  in Eq. (1) took a negative value. Note also that in the right side of Eq. (2), the second term denotes the self-demagnetization field in a grain, while the third term describes the global demagnetization field or the effective dipolar field on the grain due to other grains. The substitution of Eq. (2) to Eq. (1) yields

$$f = |\gamma|(H_{\text{FMR}} + H_k - N_0 M_r - H_{\text{ex}}). \quad (3)$$

Once the FMR field and the static properties are known,  $H_{\text{ex}}$  can be calculated using Eq. (3). The strength of  $H_{\text{ex}}$  strongly depends on  $M_r$ . When  $M_r = 0$ , about half of the grains are in the “up” state, while the other half is in the “down” state. In this case,  $H_{\text{ex}}$  is close to the intrinsic intergranular exchange field which the grains experience. When  $0 < M_r < M_s$ , more grains are in the “up” state than in the “down” state. In this scenario, among the “up” grains only those that are in close proximity to the “down” grains experience strong exchange coupling, while other grains experience a much weaker exchange field. The net effect is that the  $H_{\text{ex}}$  field calculated using Eq. (3) is an effective field averaged over the entire sample and is therefore lower than the intrinsic exchange field. Further, the closer the  $M_r$  value is to the  $M_s$  value, the smaller the  $H_{\text{ex}}$  field is. It turns out that with an increase in  $M_r$ , the  $H_{\text{ex}}$  field decreases linearly, as presented shortly. Thus, one can measure  $H_{\text{ex}}$  in different remnant states first and then plot  $H_{\text{ex}}$  as a function of  $M_r$  and extrapolate the plot to  $M_r = 0$  to determine the intrinsic intergranular exchange field. In the discussions below,  $H_{\text{ex}}$  denotes the effective exchange field at  $M_r > 0$ , while the intrinsic exchange field at  $M_r = 0$  is denoted by  $H_{\text{ex}}^0$ .

One can take the following procedures to determine the intrinsic exchange field  $H_{\text{ex}}^0$ .

- (i) Perform FMR measurements for a certain remnant state with a known  $M_r$  value, using the steps illustrated in Fig. 2(b). The measurements yield the

complex  $S_{21}$  data, which are shown by the open circles in Figs. 2(c) and 2(d). Note that the data were measured with the 10%-SiO<sub>2</sub> sample at  $f = 36$  GHz and  $M_r/M_s = 0.5$ .

- (ii) Determine  $H_{\text{FMR}}$  through fitting the real and imaginary parts of  $S_{21}$  with theoretical FMR profiles,<sup>25,26</sup> as shown by the blue curves in Figs. 2(c) and 2(d).
- (iii) Calculate  $H_{\text{ex}}$  using Eq. (3) and the  $H_{\text{FMR}}$  value from (ii).
- (iv) Repeat (i)–(iii) for different remnant states and obtain  $H_{\text{ex}}$  data for different  $M_r$  values.
- (v) Plot  $H_{\text{ex}}$  as a function of  $M_r/M_s$ , as shown in Fig. 2(e).
- (vi) Fit the  $H_{\text{ex}}$  vs.  $M_r/M_s$  data linearly and then extrapolate the line to the vertical axis to determine  $H_{\text{ex}}^0$  as shown in Fig. 2(e).

Figure 3 presents the results obtained through the measurement and analysis procedures described above. Figure 3(a) shows the  $H_{\text{ex}}$  vs.  $M_r/M_s$  data and the corresponding linear fits. One can see that all the numerical fits are reasonably good, and the  $H_{\text{ex}}$  values are all close to zero at  $M_r/M_s = 1$  as expected. The extrapolation of the lines to the  $H_{\text{ex}}$  axis yields the  $H_{\text{ex}}^0$  values for the four samples, which are presented in Fig. 3(b).

One can see three important results from the data shown in Fig. 3(b). First, the intergranular exchange field in the CoPtCr granular films with zero oxide segregant is strong, about the same as  $4\pi M_s$  and about half of  $H_k$ . Second, with the introduction of an oxide segregant to the CoPtCr films, the overall trend is that the exchange field decreases with an increase in the volume fraction  $x$  of the oxide segregant. Third, the exchange field decreases to zero when the volume fraction of the segregant is increased to 30%. This provides strong evidence for the absence of the segregant-caused splitting of the grains into smaller grains or clusters in the  $x = 30\%$  sample. Such splitting would result in an enhancement in the exchange field, rather than a decrease. These results together indicate that one can effectively manipulate the intergranular exchange coupling in PMR media via controlling the amount of the oxide segregant. They also indicate that the experimental approach described above allows for the determination of intrinsic intergranular exchange fields in granular films. It should be pointed out that, although the overall trend is that  $H_{\text{ex}}^0$  decreases with an increase in  $x$ ,  $H_{\text{ex}}^0$  increases slightly when  $x$  is increased from

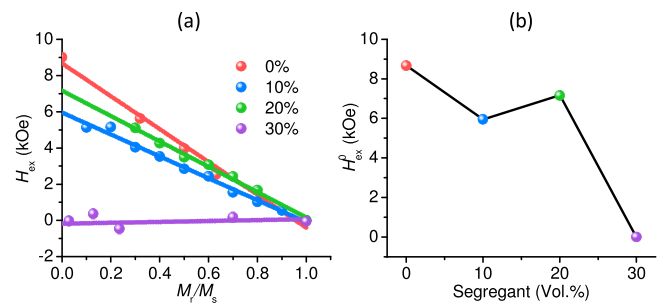


FIG. 3. Intergranular exchange field. (a) Effective exchange field  $H_{\text{ex}}$  as a function of  $M_r/M_s$  for four samples, as indicated. The dots present the data, while the lines are linear fits. (b) The intrinsic exchange field  $H_{\text{ex}}^0$ , obtained from the linear fitting shown in (a), as a function of the volume fraction of the SiO<sub>2</sub> segregant.



10% to 20%. The reason for this change is currently unknown. A simple analysis of the changes in the static properties, such as the decrease in  $H_c$  and the increase in  $4\pi M_s$ , suggests that this increase is real and not due to an experimental error. However, there are other factors, such as degraded texture, grain size, and thermal stability, which would need to be considered in detail in order to explain this  $H_{ex}^0$  increase.

For the data presented above, the CPW structure had a 50- $\mu\text{m}$ -wide signal line and a signal line-to-ground spacing of 25  $\mu\text{m}$ , the out-of-plane field used to magnetize the sample to saturation had a strength of 18 kOe, and the microwave used for the  $S_{21}$  measurements had a nominal power of 0.1 mW. All the FMR measurements were performed in a region where the magnetization was either constant or changed very little during the sweeping of the magnetic field. There are error bars in Figs. 3(a) and 3(b), but they have a size either similar to or smaller than the data points and are therefore not visible. The error bars in Fig. 3(a) are the standard deviations for the numerical fitting of the  $S_{21}$  profiles, while those in Fig. 3(b) are the standard deviations for the linear fitting of the  $H_{ex}$  vs.  $M_r/M_s$  data. The calculations of  $H_{ex}$  using Eq. (3) took  $|\gamma| = 2.8 \text{ MHz/Oe}$  and  $N_0 = 1$ .

In summary, this work studied intergranular exchange coupling in PMR media materials through FMR measurements in different magnetic states. The data showed that the exchange field in CoPtCr granular films is comparable to the saturation magnetization of the films in the absence of the oxide segregant, can be reduced through the addition of the  $\text{SiO}_2$  segregant to the films, and can be reduced to zero if the volume fraction of the  $\text{SiO}_2$  segregant is increased to 30%. The static and FMR measurements together indicate that, when the volume fraction of the segregant is as high as 30%, the segregant does not penetrate deeply into the grain cores and break the grains into smaller grains. These results contribute to the understanding of the effects of the oxide segregant on the media properties as well as on the recording performance, including thermal stability and the signal-to-noise ratio during reading. Two final notes should be made. First, the exchange field measurement approach used in this work was first used by Hinata *et al.*, though in Ref. 21 they presented only a simple comparison study on two PMR samples made using different argon pressures. Second, both the results on the effects of the oxide segregant presented above and the exchange field measurement technique used in this work should apply to future FePt-based HAMR media, though the FMR measurements have to be carried out at elevated temperatures so that the FMR frequencies can be

reduced to ease experiments and the effects at temperatures close to the writing temperature can be examined.

This work was supported mainly by Western Digital Technologies. The work was also supported partially by SHINES, an Energy Frontier Research Center funded by the U.S. Department of Energy (SC0012670), and the U.S. National Science Foundation (EFMA-1641989).

- <sup>1</sup>D. Weller, G. Parker, O. Mosendz, E. Champion, B. Stipe, X. Wang, T. Klemmer, G. Ju, and A. Ajan, *IEEE Trans. Magn.* **50**(1), 1–8 (2014).
- <sup>2</sup>L. Lu, M. Wu, M. Mallary, G. Bertero, K. Srinivasan, R. Acharya, H. Schultheiß, and A. Hoffmann, *Appl. Phys. Lett.* **103**, 042413 (2013).
- <sup>3</sup>T. Oikawa, M. Nakamura, H. Uwazumi, T. Shimatsu, H. Muraoka, and Y. Nakamura, *IEEE Trans. Magn.* **38**, 1976 (2002).
- <sup>4</sup>H. Uwazumi, T. Shimatsu, M. Terakawa, Y. Sakai, S. Takenoiri, S. Watanabe, H. Muraoka, and Y. Nakamura, *J. Magn. Soc. Jpn.* **26**, 205 (2002).
- <sup>5</sup>S. Oikawa, A. Takeo, T. Hikosaka, and Y. Tanaka, *IEEE Trans. Magn.* **36**, 2393 (2000).
- <sup>6</sup>Y. Inaba, T. Shimatsu, T. Oikawa, H. Sato, H. Aoi, H. Muraoka, and Y. Nakamura, *IEEE Trans. Magn.* **40**, 2486 (2004).
- <sup>7</sup>T. Shimatsu, H. Uwazumi, H. Muraoka, and Y. Nakamura, *IEEE Trans. Magn.* **38**, 1973 (2002).
- <sup>8</sup>H. Uwazumi, K. Enomoto, Y. Sakai, S. Takenoiri, T. Oikawa, and S. Watanabe, *IEEE Trans. Magn.* **39**, 1914 (2003).
- <sup>9</sup>I. Tagawa and Y. Nakamura, *IEEE Trans. Magn.* **27**, 4975 (1991).
- <sup>10</sup>T. Shimatsu, T. Kondo, K. Mitsuzuka, S. Watanabe, H. Aoi, H. Muraoka, and Y. Nakamura, *IEEE Trans. Magn.* **43**, 2091 (2007).
- <sup>11</sup>Y. Liu, K. Dahmen, and A. Berger, *Phys. Rev. B* **77**, 054422 (2008).
- <sup>12</sup>C. Papusoi, K. Srinivasan, and R. Acharya, *J. Appl. Phys.* **110**, 083908 (2011).
- <sup>13</sup>M. El-Hilo, K. O'Grady, P. I. Mayo, R. W. Chantrell, I. L. Sanders, and J. K. Howard, *IEEE Trans. Magn.* **28**, 3282 (1992).
- <sup>14</sup>J. P. C. Bernard and H. Cramer, *J. Magn. Magn. Mater.* **120**, 221 (1993).
- <sup>15</sup>H. Uwazumi, T. Shimatsu, and Y. Kuboki, *J. Appl. Phys.* **91**, 7095 (2002).
- <sup>16</sup>O. Hovorka, Y. Liu, K. A. Dahmen, and A. Berger, *Appl. Phys. Lett.* **95**, 192504 (2009).
- <sup>17</sup>R. J. M. van de Veerdonk, X. Wu, and D. Weller, *IEEE Trans. Magn.* **39**, 590 (2003).
- <sup>18</sup>A. Berger, Y. Xu, B. Lengsfeld, Y. Ikeda, and E. E. Fullerton, *IEEE Trans. Magn.* **41**, 3178 (2005).
- <sup>19</sup>J. Wu, L. Holloway, H. Laidler, K. O'Grady, S. Khizroev, J. K. Howard, R. W. Gustafson, and D. Litvinov, *IEEE Trans. Magn.* **38**, 1682 (2002).
- <sup>20</sup>S. Hinata, S. Saito, N. Itagaki, and M. Takahashi, *IEEE Trans. Magn.* **48**, 1248 (2012).
- <sup>21</sup>S. Hinata, S. Saito, and M. Takahashi, *IEEE Trans. Magn.* **48**, 3177 (2012).
- <sup>22</sup>M. Zheng, B. R. Acharya, G. Choe, J. N. Zhou, Z. D. Yang, E. N. Abarra, and K. E. Johnson, *IEEE Trans. Magn.* **40**, 2498 (2004).
- <sup>23</sup>T. Shimatsu, H. Sato, T. Oikawa, Y. Inaba, O. Kitakami, S. Okamoto, H. Aoi, H. Muraoka, and Y. Nakamura, *IEEE Trans. Magn.* **41**, 566 (2005).
- <sup>24</sup>D. Laughlin, N. Nuhfer, S. Park, H. Yuan, and J. Zhu, *J. Appl. Phys.* **105**, 07B739 (2009).
- <sup>25</sup>Y. Ding, T. J. Klemmer, and T. M. Crawford, *J. Appl. Phys.* **96**, 2969 (2004).
- <sup>26</sup>H. T. Nembach, T. J. Silva, J. M. Shaw, M. L. Schneider, M. J. Carey, S. Maat, and J. R. Childress, *Phys. Rev. B* **84**, 054424 (2011).